nature medicine

SUPPLEMENTARY INFORMATION

https://doi.org/10.1038/s41591-019-0368-8

In the format provided by the authors and unedited.

Combination of ERK and autophagy inhibition as a treatment approach for pancreatic cancer

Kirsten L. Bryant[1], Clint A. Stalnecker[1], Daniel Zeitouni[1], Jennifer E. Klomp[1], Sen Peng[2], Andrey P. Tikunov[3], Venugopal Gunda[4], Mariaelena Pierobon[5], Andrew M. Waters[1], Samuel D. George[1], Garima Tomar[1], Björn Papke[1], G. Aaron Hobbs[1], Liang Yan[6], Tikvah K. Hayes[7], J. Nathaniel Diehl[7], Gennifer D. Goode[4], Nina V. Chaika[4], Yingxue Wang[8], Guo-Fang Zhang[8], Agnieszka K. Witkiewicz[9], Erik S. Knudsen[10], Emanuel F. Petricoin III[5], Pankaj K. Singh[4], Jeffrey M. Macdonald[3], Nhan L. Tran[11], Costas A. Lyssiotis[12], Haoqiang Ying[6], Alec C. Kimmelman[13], Adrienne D. Cox[1,14,15] and Channing J. Der[1,7,15]*

[1]Lineberger Comprehensive Cancer Center, University of North Carolina at Chapel Hill, Chapel Hill, NC, USA. [2]Cancer and Cell Biology Division, Translational Genomics Research Institute, Phoenix, AZ, USA. [3]Biomedical Engineering, University of North Carolina at Chapel Hill, Chapel Hill, NC, USA. [4]Eppley Institute for Cancer Research, University of Nebraska Medical Center, Omaha, NE, USA. [5]Center for Applied Proteomics and Molecular Medicine, George Mason University, Fairfax, VA, USA. [6]Department of Molecular and Cellular Oncology, Division of Basic Science Research, The University of Texas MD Anderson Cancer Center, Houston, TX, USA. [7]Curriculum in Genetics and Molecular Biology, University of North Carolina at Chapel Hill, Chapel Hill, NC, USA. [8]Sarah W. Stedman Nutrition and Metabolism Center & Duke Molecular Physiology Institute, Department of Medicine, Duke University, Durham, NC, USA. [9]Center for Personalized Medicine, Roswell Park Cancer Center, Buffalo, NY, USA. [10]Department of Molecular and Cell Biology, Roswell Park Cancer Center, Buffalo, NY, USA. [11]Department of Cancer Biology, Mayo Clinic, Phoenix, AZ, USA. [12]Department of Molecular and Integrative Physiology; Department of Internal Medicine, Division of Gastroenterology and University of Michigan Comprehensive Cancer Center, Ann Arbor, MI, USA. [13]Perlmutter Cancer Center, NYU Langone Medical Center, New York City, NY, USA. [14]Department of Radiation Oncology, University of North Carolina at Chapel Hill, Chapel Hill, NC, USA. [15]Department of Pharmacology, University of North Carolina at Chapel Hill, Chapel Hill, NC, USA.
*e-mail: cjder@med.unc.edu

Supplementary Figure 1a-d

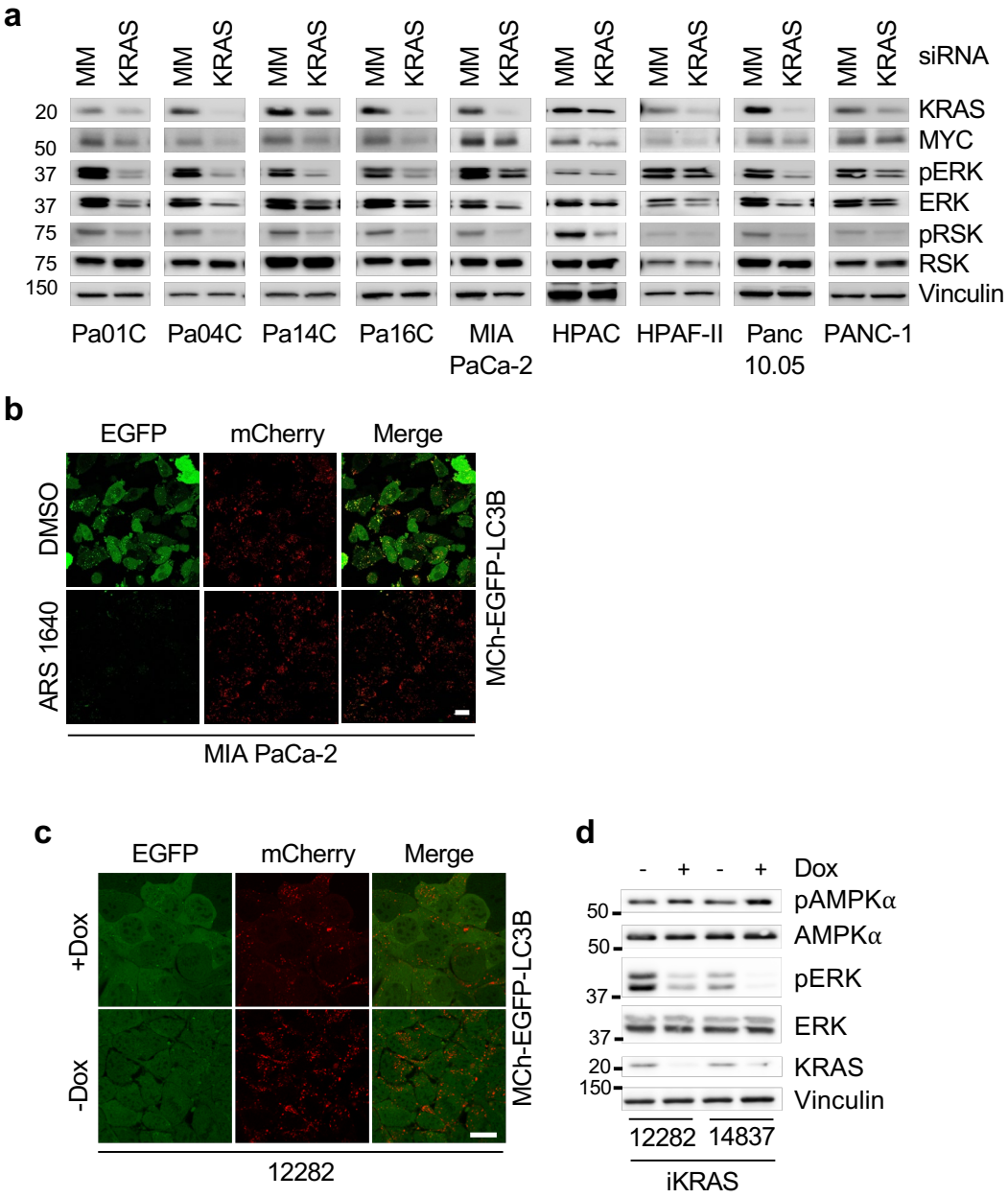

Supplementary Figure 1e-k

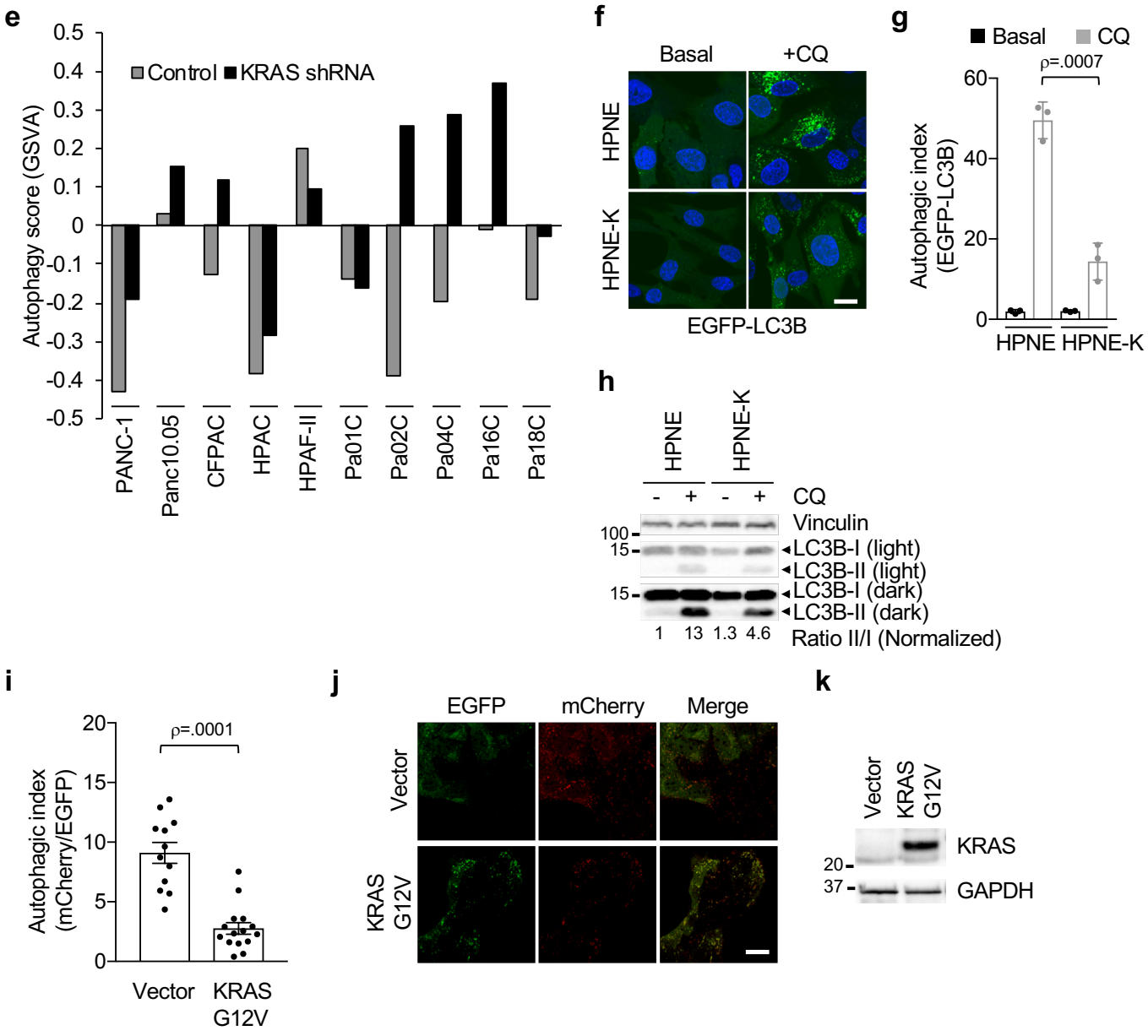

Supplementary Figure 1 | Genetic suppression of mutant KRAS increases autophagic flux in PDAC cell lines. a, Immunoblots of cell lines analyzed in Fig. 1a-c showing relative KRAS levels pre- and post- siRNA mediated knockdown. MYC, pERK, total ERK and pRSK, and total RSK were probed to assess downstream signaling, and vinculin was probed to show total protein. Data for HPAC, PANC-1, MIA PaCa-2, Pa01C, and Pa14C are representative of two independent experiments and for HPAF-II, Pa04C, and Pa16C cells, one independent experiment. **b**, Representative images corresponding to Fig. 1c. **c**, Representative images of cells described and quantified in (Fig. 1e). Scale bar = 20 μm. **d**, iKRAS cells were treated as shown to deplete KRAS (Dox) or inhibit autophagic flux (Baf) and immunoblots were done to determine the levels of phosphorylated AMPKα (pAMPKα), total AMPKα, KRAS, and vinculin, representative of three independent experiments. **e**, A panel of 10 PDAC cell lines was stably transduced with shRNA targeting *KRAS* (KRAS shRNA) or a nonspecific control (Control) for 72-120 h. Cells were collected and RNA-Seq analysis was performed. GSVA was performed in order to estimate the variation of different metabolic pathway activities upon KRAS KD in a non-supervised manner. Shown are GSVA scores for a panel of autophagy-related genes. **f,** Control and $KRAS^{G12V}$-transformed human pancreatic nestin-expressing cells (HPNE and HPNE-K, respectively) were infected with a lentiviral vector to stably express EGFP-LC3B. Representative images of cells treated with and without chloroquine (CQ, 16 h) to monitor autophagic flux. Blue: DAPI. **g**, Quantification of EGFP positive punctae area normalized to cell area (autophagic index). Mean autophagic index is plotted, with each individual data point representing one field containing at least ten analyzed cells. Data shown are the average of three biological replicates, ρ values from two-sided, unpaired t-test, comparing average autophagic index across three replicates following CQ treatment, error bars denote S.E.M. **h**, Immunoblot analyses of cell lysates from control HPNE and $KRAS^{G12V}$-transformed HPNE (HPNE-K) cells treated with or without CQ (16 h) were done

to determine the levels of LC3B and vinculin. **i**, RIE-1 cells stably expressing EGFP-mCherry-LC3B were subsequently stably infected with KRAS ^{G12V} or empty vector and autophagic flux was assessed. Mean autophagic index is plotted, with each individual data point representing one field containing at least ten analyzed cells. Data are representative of two biological replicates, ρ value from two-sided, unpaired *t*-test, error bars: S.E.M. **j**, Representative images of cells quantified in (**i**). **k**, Immunoblot analysis demonstrating relative KRAS levels among mutants, GAPDH shows total protein is representative of two independent experiments.

Supplementary Figure 2a

a

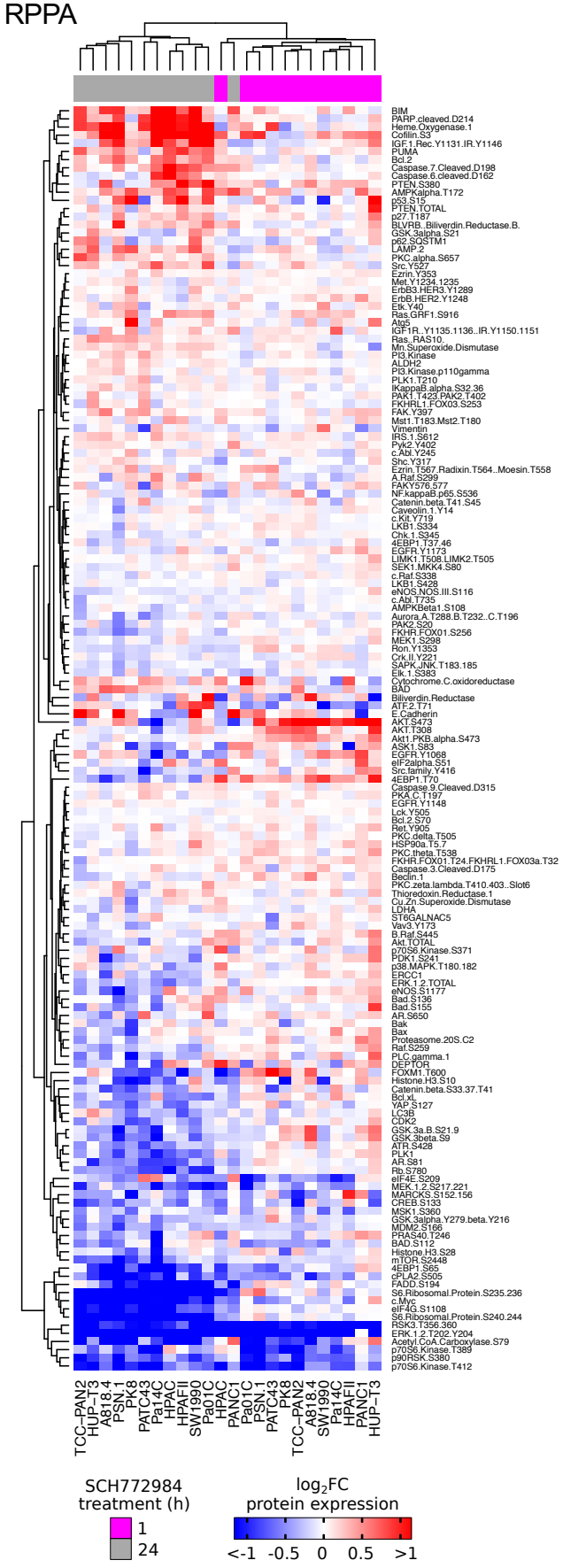

Supplementary Figure 2b

b

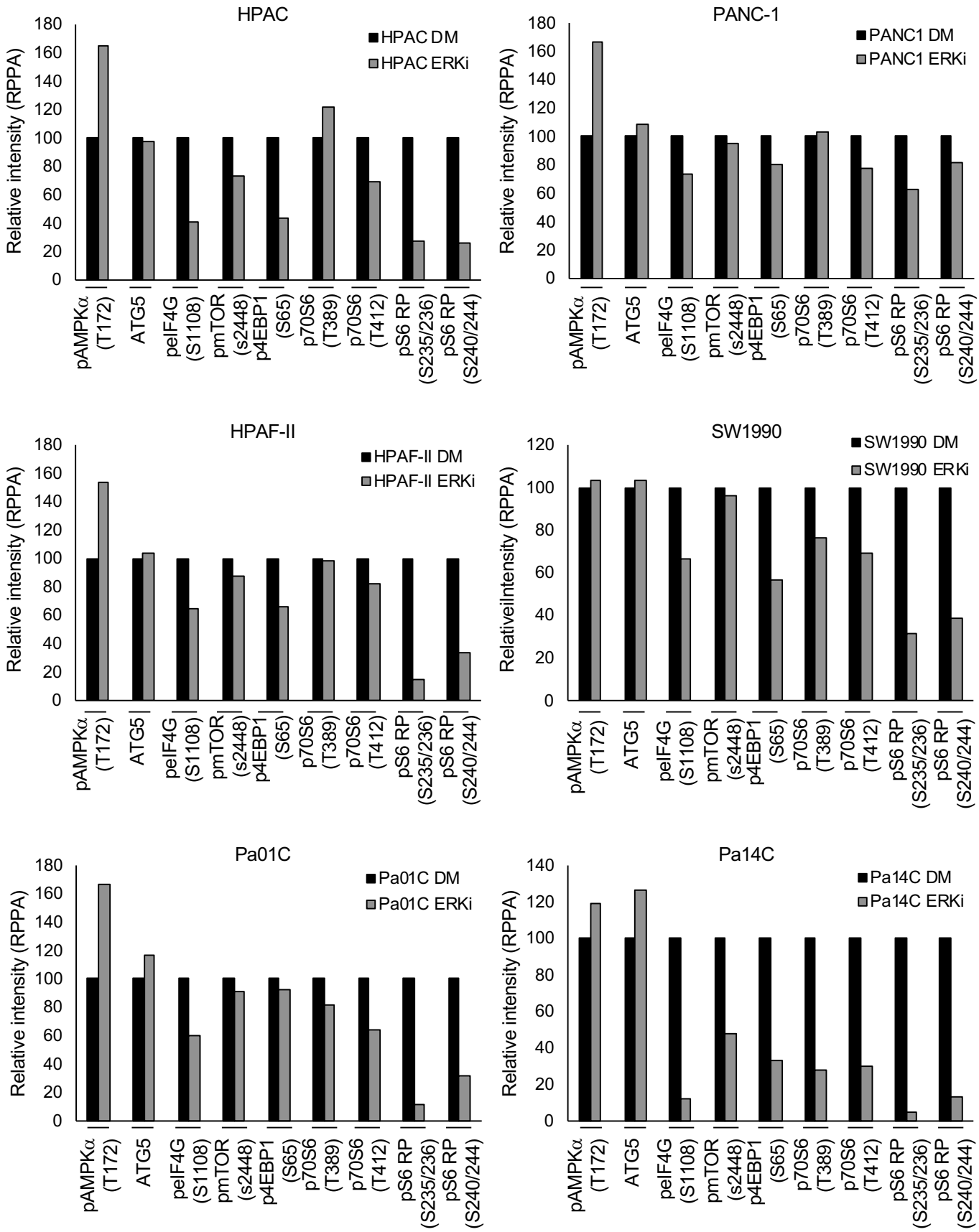

Supplementary 2b continued

b, contin.

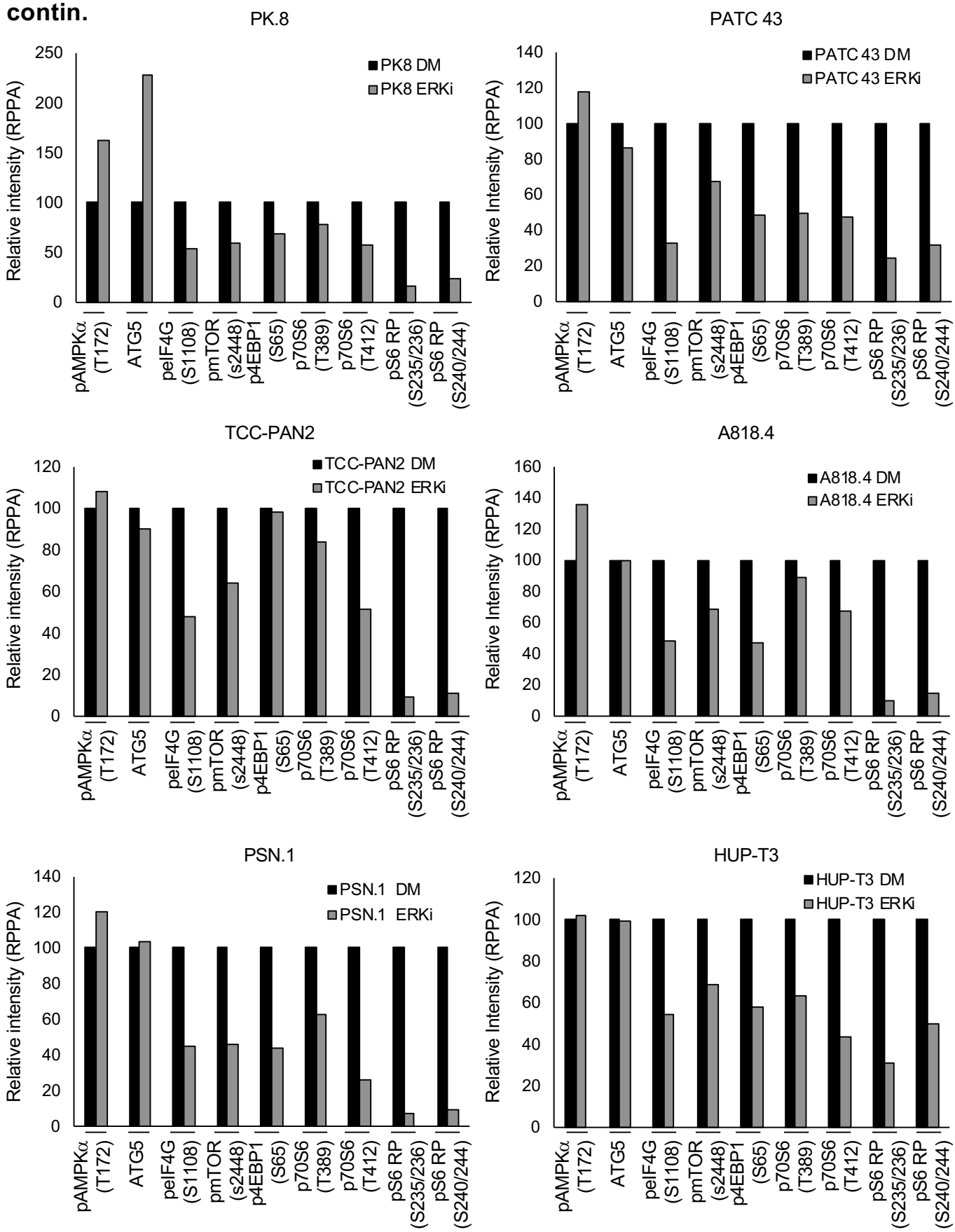

Supplementary Figure 2c

c

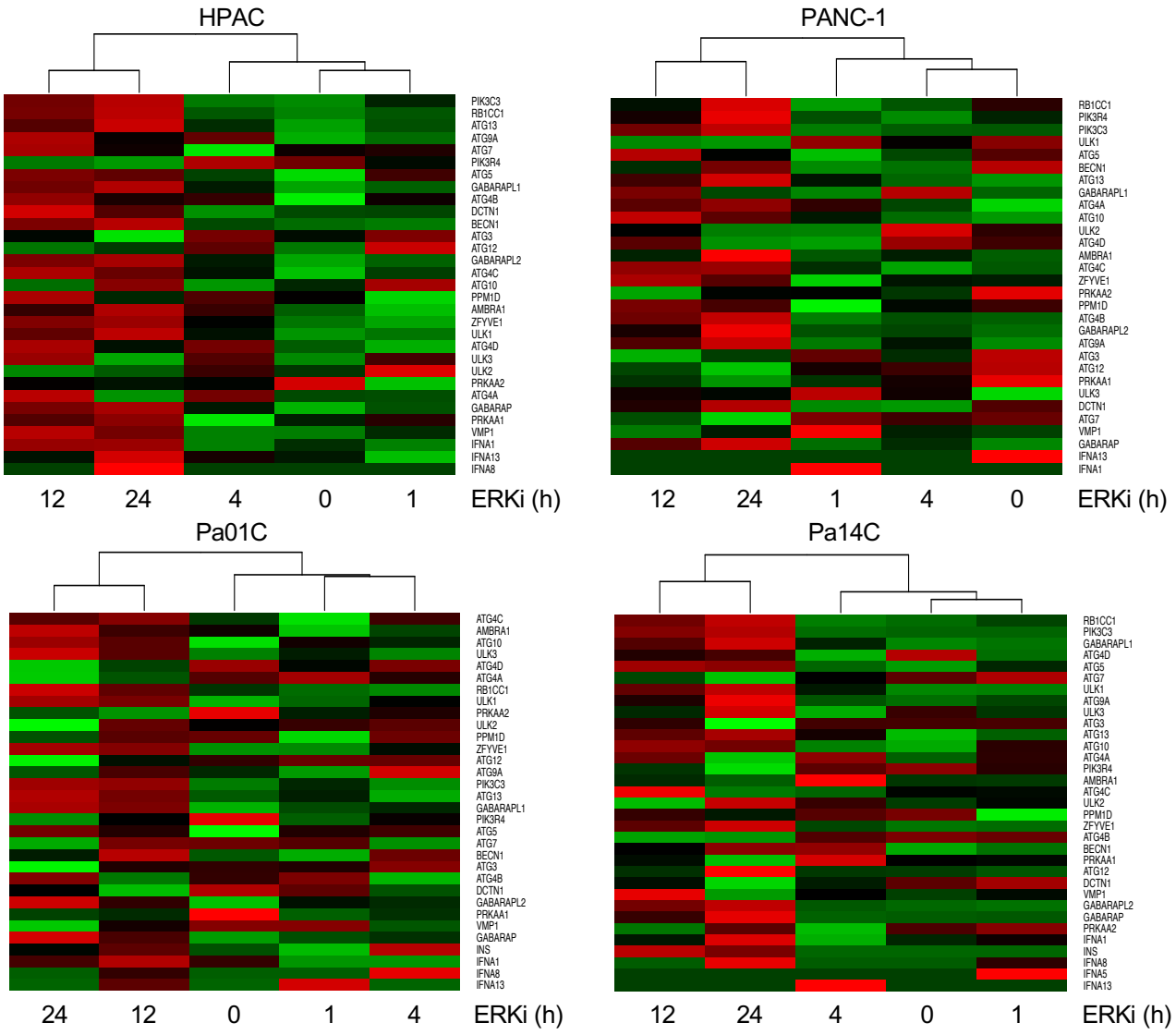

Supplementary Figure 2 | ERK inhibition influences the transcription and activation of upstream mediators of autophagic signaling. a, PDAC cell lines were treated with SCH772984 (ERKi, 1 μM) or vehicle control (DMSO) for 1 or 24 h. Three biological replicates were prepared and Reverse-phase protein array (RPPA) analysis was performed. RPPA expression data for 1 h of SCH772984 treatment were standardized to no treatment samples and 24 h SCH772984 treatment samples were standardized to 24 h DMSO treated samples. Data were log2 transformed and medians of three biological replicates are represented in the heat map. Red signal denotes higher expression relative to the median expression level within the group and blue signal denotes lower expression relative to the mean expression level within the group. Samples and proteins were arranged via hierarchical clustering. **b**, RPPA relative intensity data for each individual cell line represented in Fig. 3b. **c**, Heat maps from four of the seven cell lines analyzed in Fig. 3d of autophagy-related genes, duration of treatment with SCH772984 (ERKi) denoted at the bottom of each column. Expression levels shown are representative of log2 values. Unsupervised hierarchical clustering analysis was performed to order columns in heat maps where red signal denotes higher expression relative to the mean expression level within the group and green signal denotes lower expression relative to the mean expression level within the group.

Supplementary Figure 3a-b

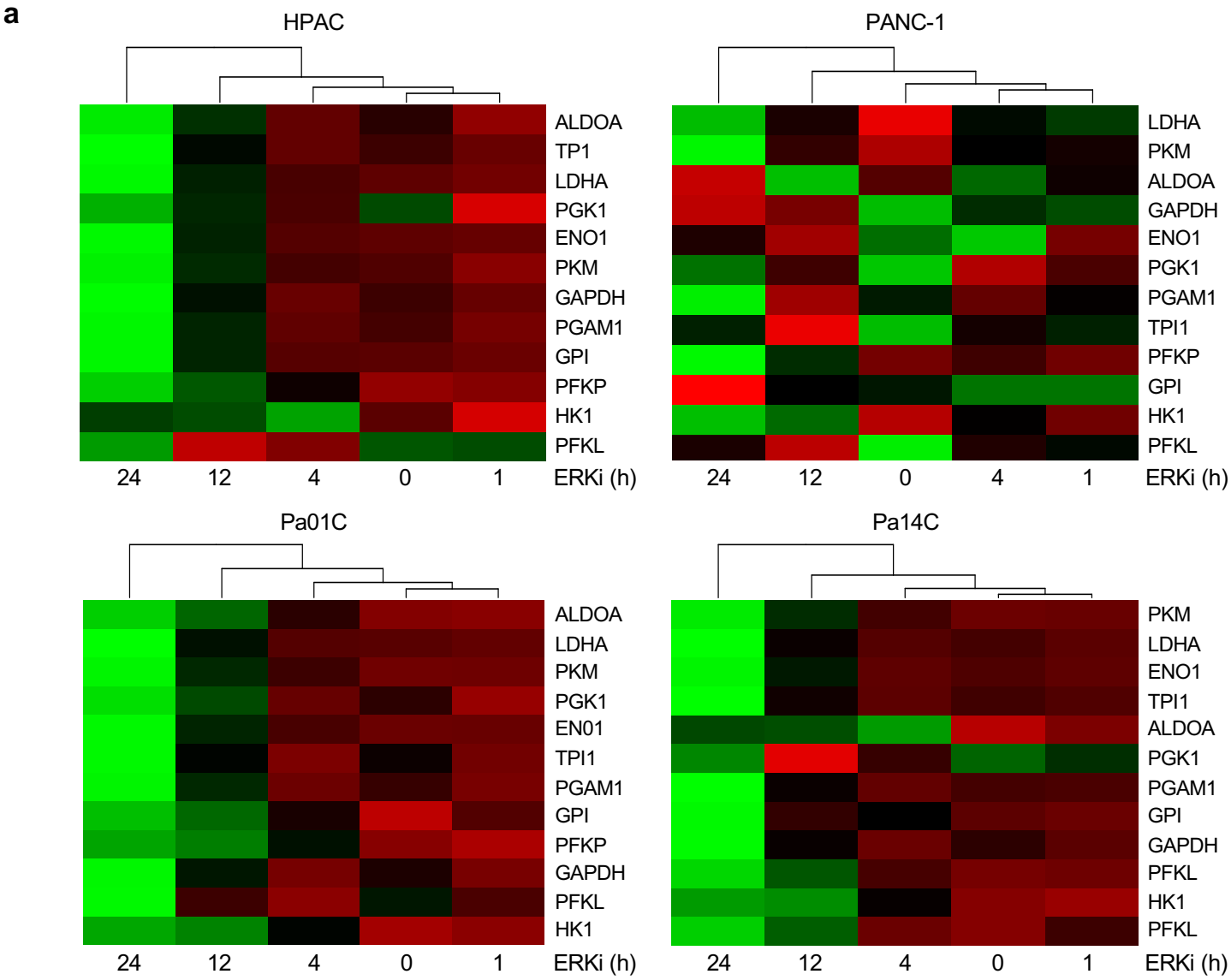

Supplementary Figure 3c-f

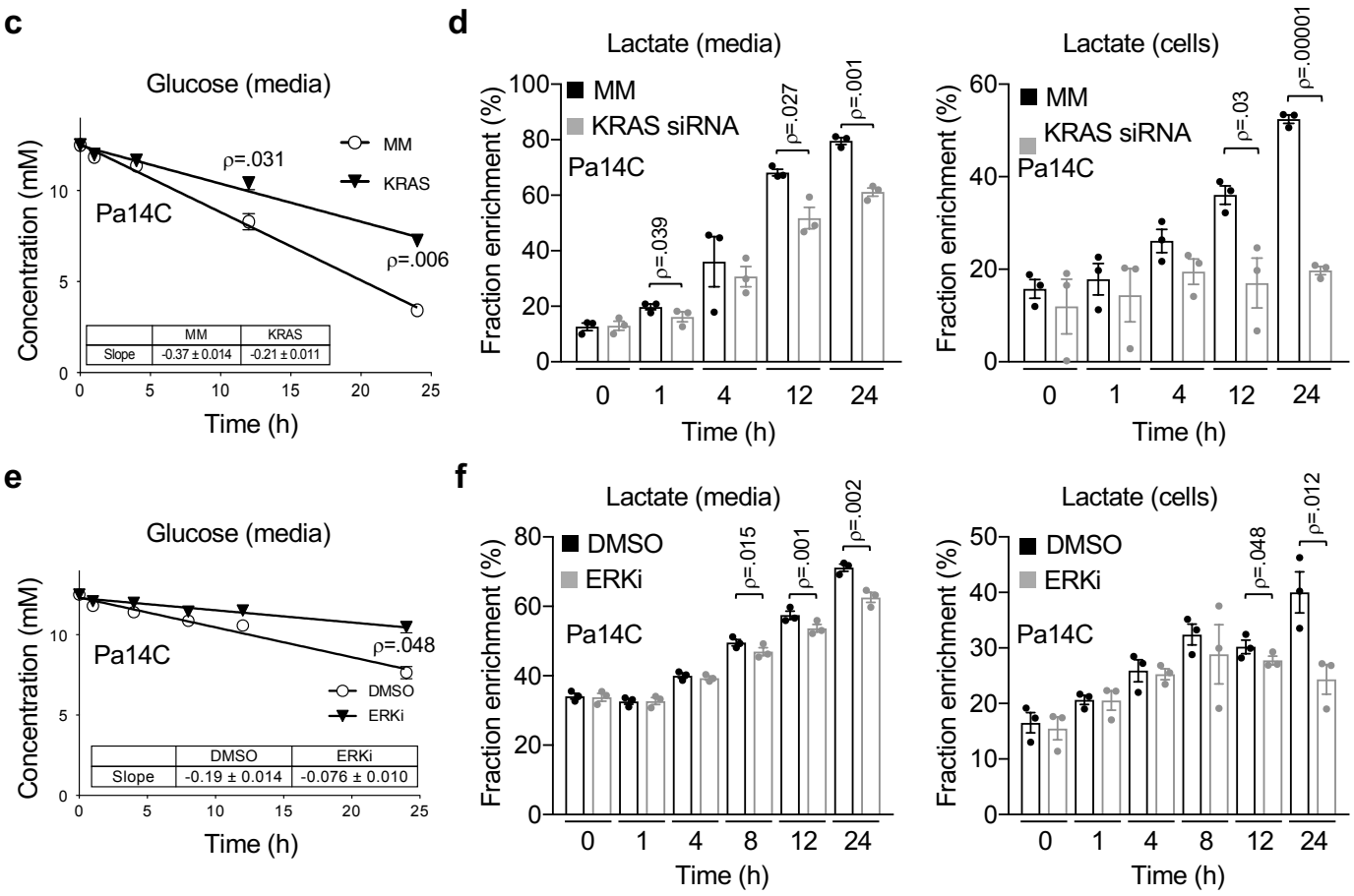

Supplementary Figure 3g-h

g

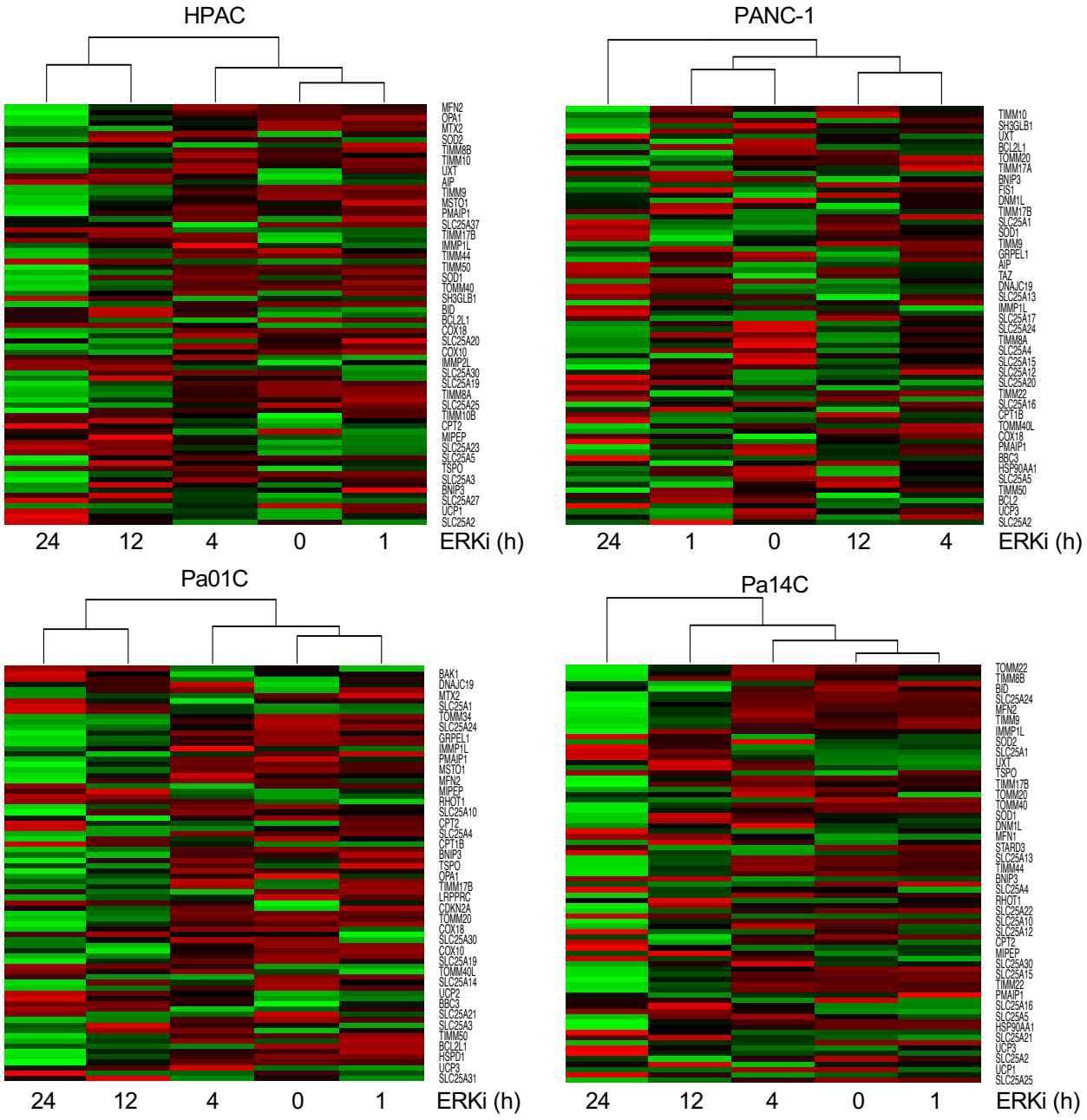

h

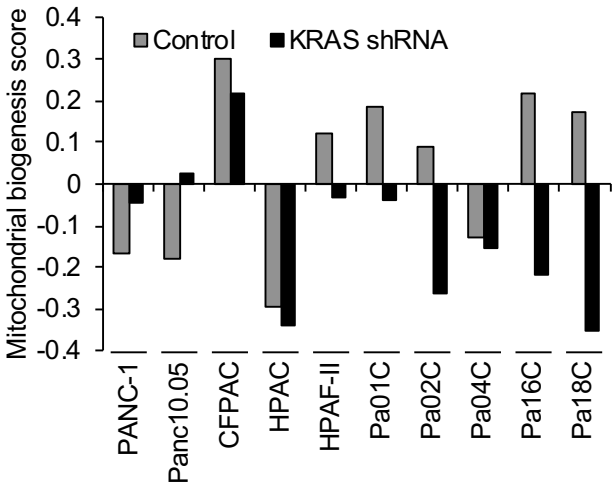

Supplementary Figure 3i-l

i

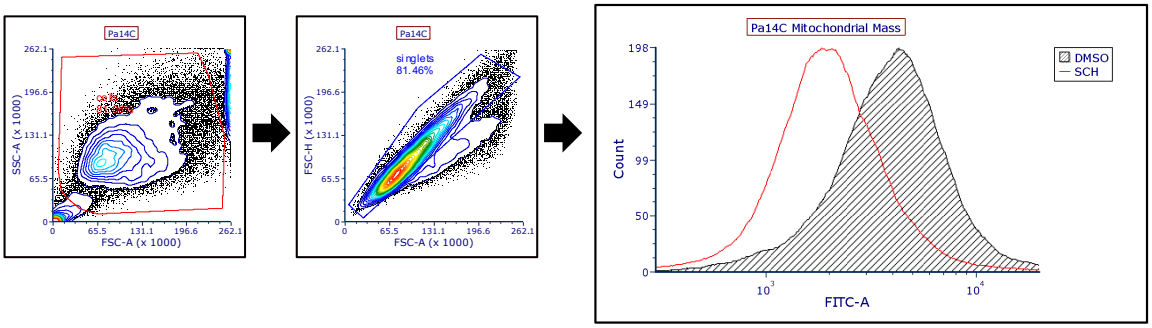

Filename	Median	CV
Pa14C_DMSO_001.fcs	3604.56	96.01
Pa14C_SCH_002.fcs	1777.92	103.60

j

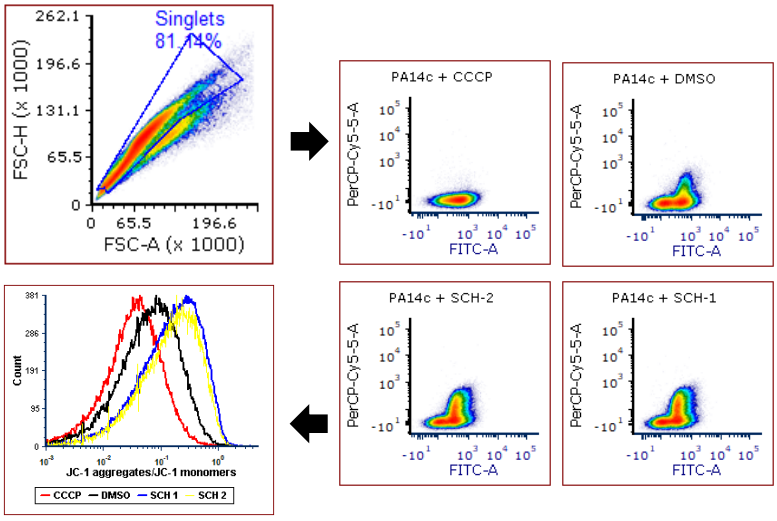

k

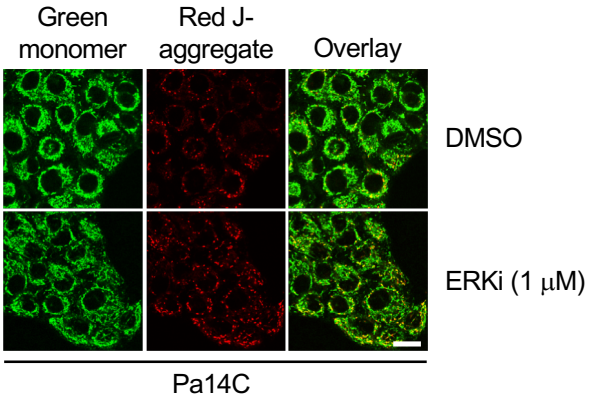

Histogram #	Filename	# of Events	Median
1	Pa14-1_DMSO + CCCP_001.fcs compensated Parameter Math applied	93151	0.012
2	Pa14-1_DMSO_002.fcs compensated Parameter Math applied	94998	0.026
3	Pa14-1_SCH-1_003.fcs compensated Parameter Math applied	94262	0.105
4	Pa14-1_SCH-2_004.fcs compensated Parameter Math applied	94322	0.105

l

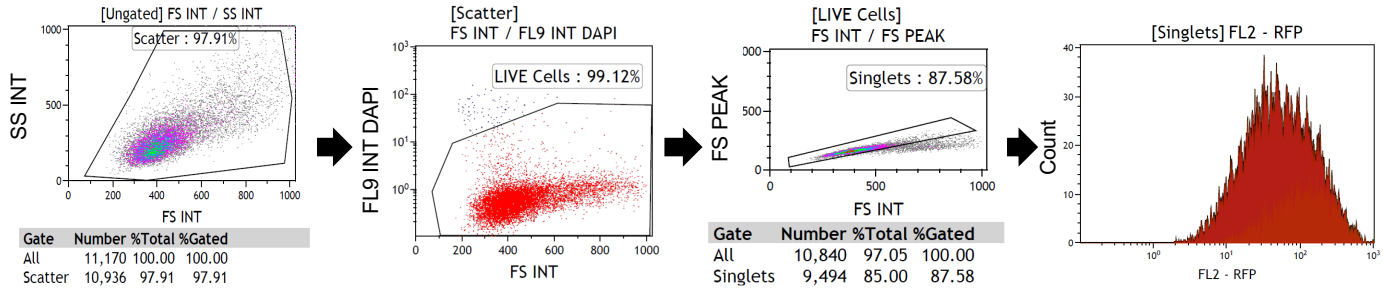

Gate	Number	%Total	%Gated
All	11,170	100.00	100.00
Scatter	10,936	97.91	97.91

Gate	Number	%Total	%Gated
All	10,840	97.05	100.00
Singlets	9,494	85.00	87.58

Supplementary Figure 3m-n

m

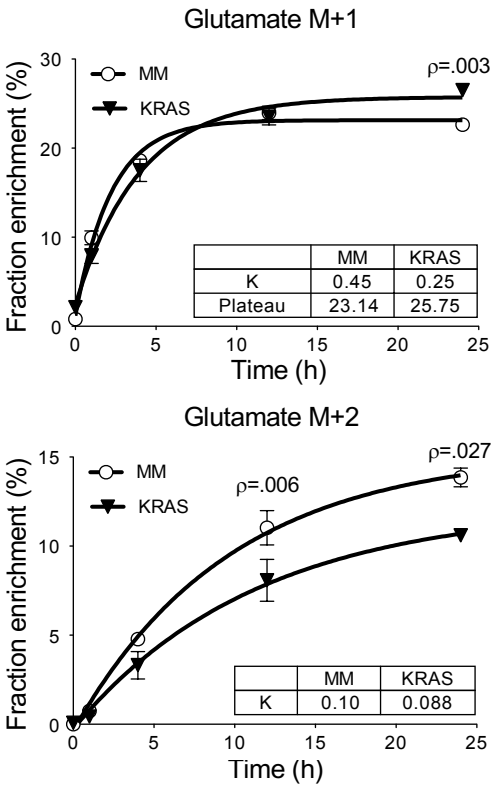

n

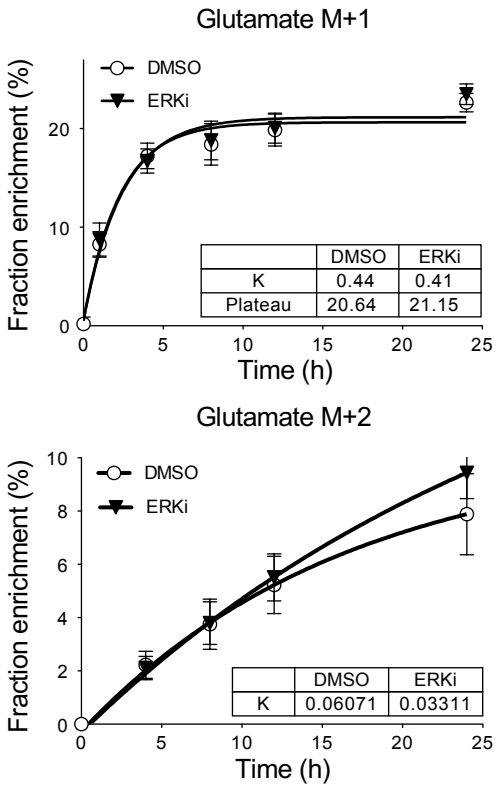

Supplementary Figure 3 | Genetic silencing of KRAS and ERK inhibition reduces glycolytic flux and mitochondrial function in PDAC. a, Heat maps from four of the seven cell lines analyzed in Fig. 3f of glycolysis-related genes, duration of treatment with SCH772984 (ERKi) denoted at the bottom of each column. Heat maps generated as in (Extended Data Fig. 3g). **b**, A panel of 10 PDAC cell lines were stably transduced with shRNA targeting *KRAS* (KRAS shRNA) or a nonspecific control (Control) for 72-120 h. Cells were collected and RNA-Seq analysis was performed. GSVA was performed in order to estimate the variation of different metabolic pathway activities upon KRAS KD in a non-supervised manner. Shown are GSVA scores for a panel of glycolysis-related genes. **c**, Pa14C cells were transiently transfected with siRNA targeting KRAS (KRAS) or a mismatch control (MM). Following 48 h, medium was changed to that containing 1,6-$^{13}C_2$-labeled glucose (12.5 mM) and metabolic flux analysis was performed over a 24 h time course. Shown is average glucose concentration in media across three independent experiments, ρ values from two-sided, unpaired t-test, error bars denote S.D. Slope is average across three independent experiments and error is S.D. **d**, Samples were prepared as described in (**c**), shown is average fraction enrichment of lactate in media and cells over time across three independent experiments, ρ values from two-sided, unpaired t-test, error bars denote S.E.M. **e,** Pa14C cells were treated with SCH772984 (ERKi, 1 μM) or vehicle control (DMSO) for 24 h. Upon ERKi treatment, medium was changed to that containing 1,6-$^{13}C_2$-labeled glucose (12.5 mM) and metabolic flux analysis was performed over a 24 h time course. Shown is average glucose concentration in media across three independent experiments, ρ values from two-sided, unpaired t-test, error bars denote S.D. Slope is average across three independent experiments and error is S.D. **f**, Samples were prepared as described in (**e**), shown is average fraction enrichment of lactate in media and cells over time across three independent experiments, ρ values from two-sided, unpaired t-test, error bars denote S.E.M. **g,** Heat maps representing four of the seven cell lines

analyzed in Fig. 3g of mitochondrial biogenesis-related genes, duration of treatment with SCH772984 (ERKi) denoted at the bottom of each column. Heat maps generated as in Extended Data Fig. 3g. **h**, A panel of 10 PDAC cell lines were stably transduced with shRNA targeting KRAS (KRAS shRNA) or a nonspecific control (Control) for 72-120 h. Cells were collected and RNA-Seq analysis was performed. GSVA was performed in order to estimate the variation of different metabolic pathway activities upon KRAS KD in a non-supervised manner. Shown are GSVA scores for a panel of mitochondrial biogenesis-related genes. **i**, Gating strategy for mitochondrial mass experiments described in Fig. 4a. **j**, Gating strategy for quantification of relative mitochondrial potential in human PDAC cell lines via labeling with the JC-1 mitochondrial dye described in Fig. 4i-j. **k**, Representative images of Pa14C cells treated and labeled as described in Fig. 4i. Green: JC-1 monomers; Red: J-aggregates; Scale bar = 20 μm, images are representative of three independent experiments. **l**, Gating strategy for quantification of relative mitochondrial potential in iKRAS cells using TMRE described in Extended Data Fig. 6a. **m**, Pa14C cells were transiently transfected with siRNA targeting *KRA*S (KRAS) or a MM control. Following 48 h, media was changed to that containing 1,6-^{13}C-labeled glucose (12.5 mM) and metabolic flux analysis was performed over a 24 h time course. Shown is the average isotopomer distribution for glutamate over time across three independent experiments, ρ values from two-sided, unpaired t-test, error bars denote S.E.M. R^2 values for curve fits are 0.9857 (MM, M+1), 0.9806 (K1, M+1), 0.9804 (MM, M+2), 0.9533 (K1, M+2)). **n**, Pa14C cells were treated with SCH772984 (ERKi) for a time course of 24 h. Upon the addition of SCH772984 (ERKi), media was changed to that containing 1,6-$^{13}C_2$-labeled glucose (12.5 mM) and metabolic flux analysis was performed over a 24 h time course. Shown is the average isotoplogue distribution for glutamate in the media over time across three independent experiments, error bars denote S.E.M. R^2 values for curve fits are 0.9189 (DMSO, M+1), 0.9129 (ERKi, M+1), 0.8336 (DMSO, M+2), 0.9235 (ERKi, M+2)).

Supplementary Figure 4a-b

a

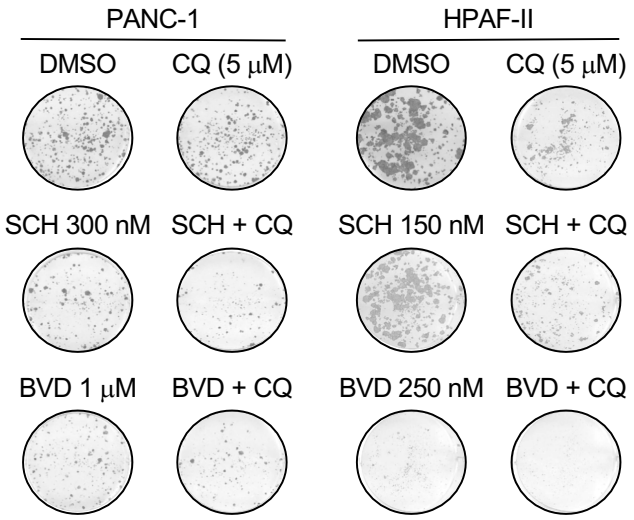

b

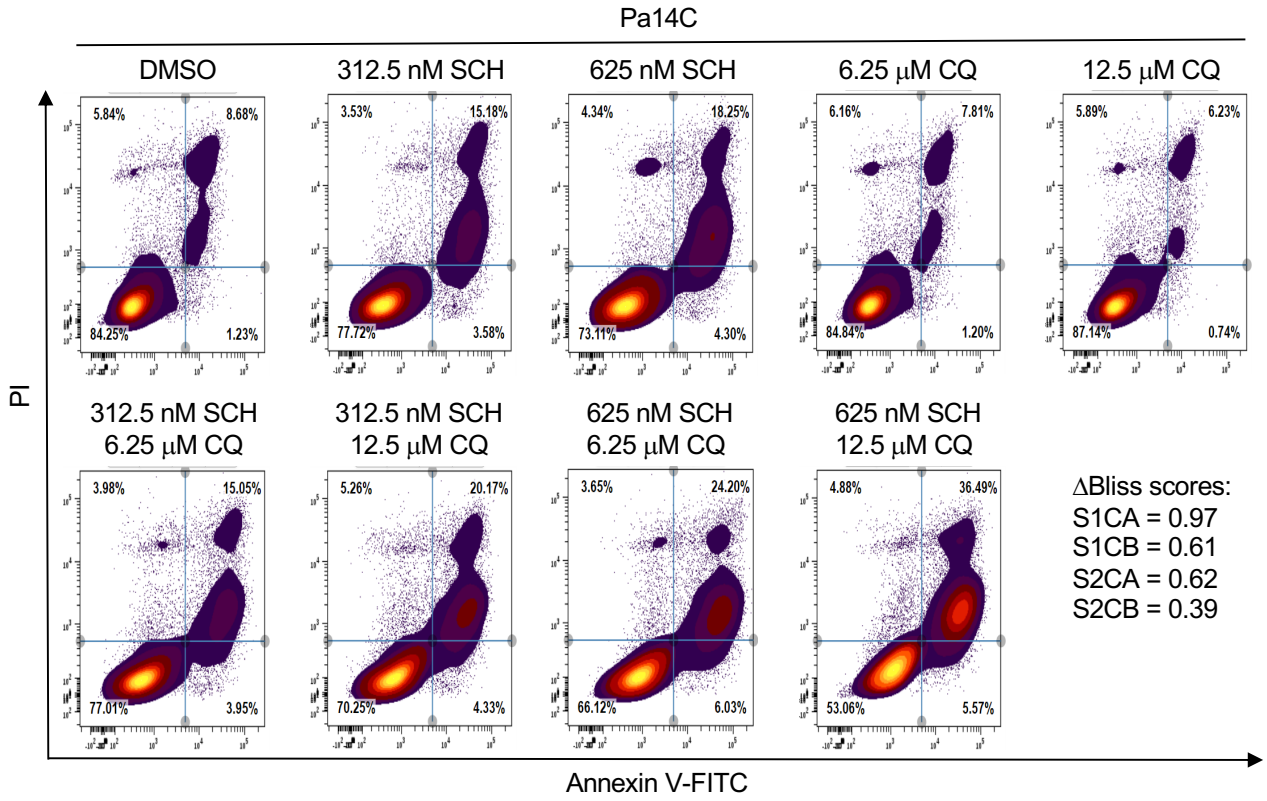

Supplementary Figure 4c-e

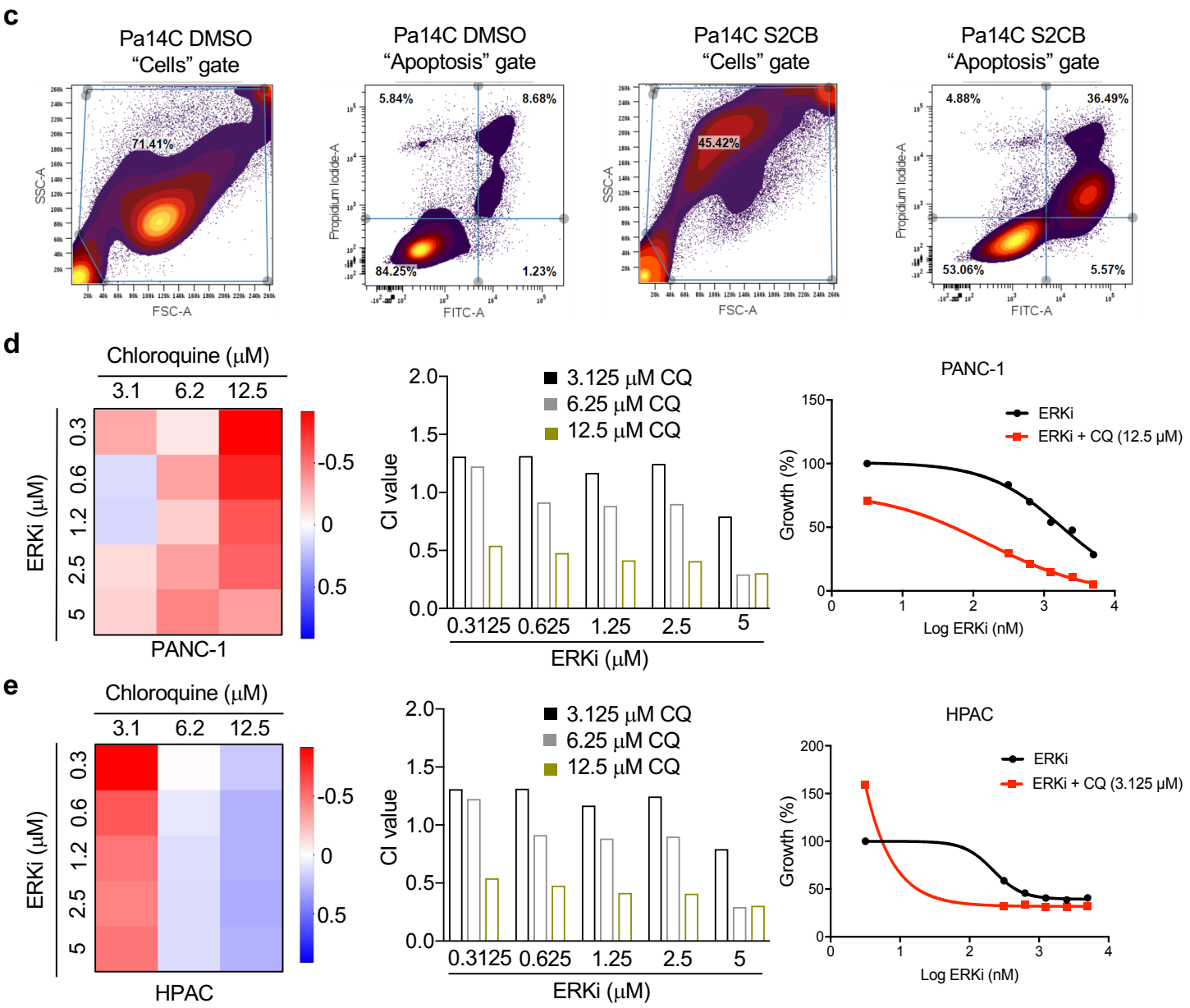

Supplementary Figure 4 | ERK inhibition synergizes with the inhibition of autophagy to reduce proliferation in human PDAC cells.

a, Representative images of colony formation assays in PANC-1 and HPAF-II cell lines quantified in Fig. 5b. Data are representative of two independent experiments. **b**, Representative contour plots from apoptosis experiment in Pa14C cell line described in Fig. 5d. **c**, Gating strategy for Annexin-V apoptosis experiments described in Fig. 5d and (**b**). **d**, PANC-1 cells were grown as matrix embedded spheroids for 10 d in the presence of indicated concentrations of chloroquine (CQ) and SCH772984 (ERKi). Shown on the left is a heatmap representing BLISS independence scores, next are CI values calculated using Compusyn, and on the right are growth curves representing the most synergistic CQ concentration. **e**, HPAC cells were grown, treated, and analyzed as described in (**d**).

Supplementary Figure 5

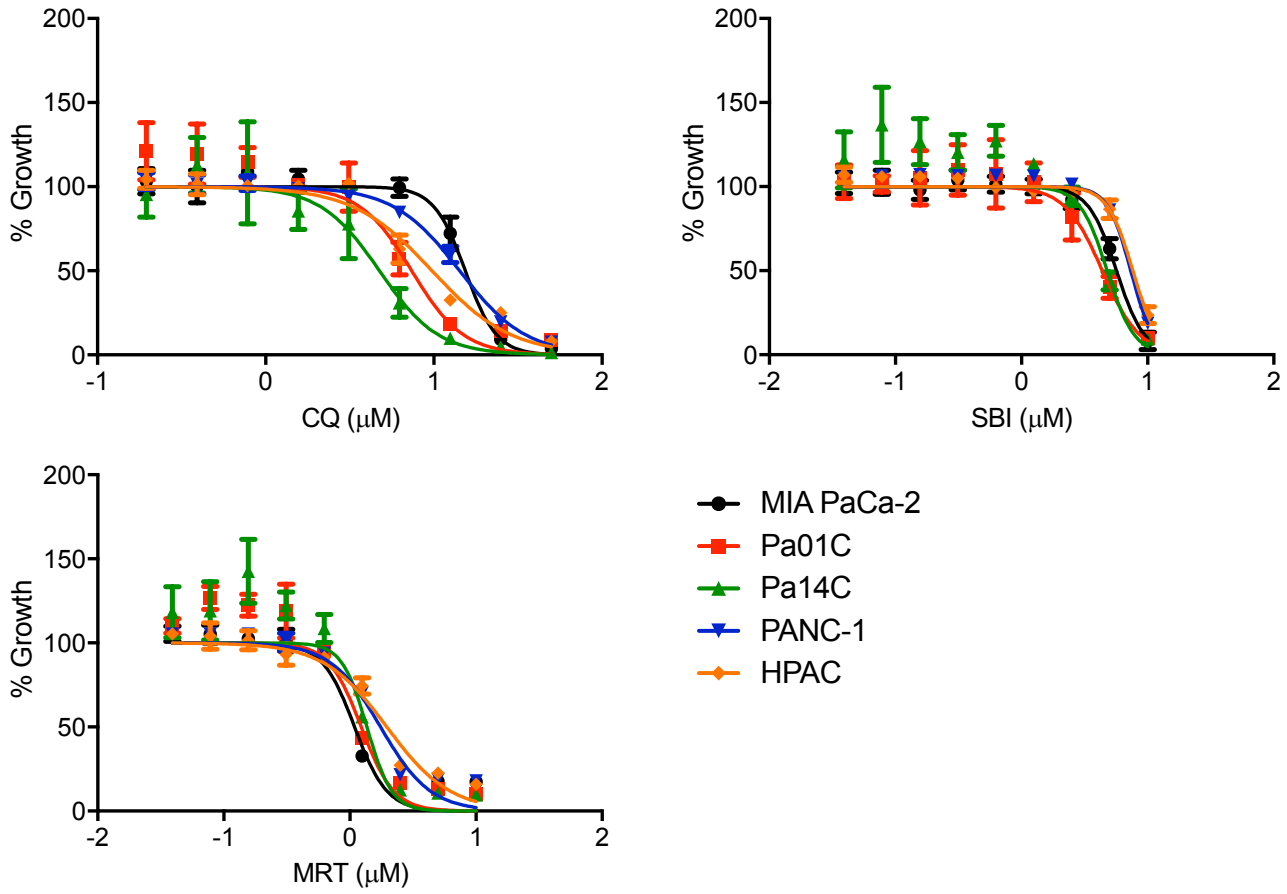

Supplementary Figure 5| Comparison of the sensitivity of PDAC cell lines to different autophagy inhibitors. Dose response curves for a panel of PDAC cell lines treated with a range of chloroquine (CQ), SBI-0206965 (SBI), or MRT68921 (MRT) concentrations for 5 d, proliferation was assessed by live cell counting. Normalized mean cell number, comparing treatment conditions to DMSO control, which was normalized to 100, is plotted and error bars denote S.D. of three technical replicates. Curves are representative of three independent experiments.

Table S1. Gene sets used for Gene Set Variation Analyses

Gene	Pathway
RB1CC1	Autophagy
GABARAPL2	Autophagy
ATG5	Autophagy
VMP1	Autophagy
PIK3C3	Autophagy
ULK2	Autophagy
ATG4A	Autophagy
AMBRA1	Autophagy
IFNA8	Autophagy
ATG4C	Autophagy
BECN1	Autophagy
ATG4D	Autophagy
PRKAA1	Autophagy
GABARAPL1	Autophagy
ULK3	Autophagy
ATG3	Autophagy
ATG12	Autophagy
IFNA5	Autophagy
ATG10	Autophagy
PRKAA2	Autophagy
ZFYVE1	Autophagy
ATG4B	Autophagy
GABARAP	Autophagy
PPM1D	Autophagy
ATG13	Autophagy
ULK1	Autophagy
PIK3R4	Autophagy
ATG7	Autophagy
IFNA1	Autophagy
ATG9A	Autophagy
DCTN1	Autophagy
IFNA13	Autophagy
INS	Autophagy
M6PR	Lysosome
LAMP2	Lysosome
IDS	Lysosome
SLC11A1	Lysosome

ATP6V0A1	Lysosome
AGA	Lysosome
CTNS	Lysosome
ATP6V1H	Lysosome
HEXB	Lysosome
GALC	Lysosome
CTSA	Lysosome
AP3D1	Lysosome
LAPTM4A	Lysosome
CLTCL1	Lysosome
AP3M2	Lysosome
ATP6AP1	Lysosome
AP1M1	Lysosome
LAMP3	Lysosome
AP4E1	Lysosome
GNPTG	Lysosome
MCOLN1	Lysosome
GGA1	Lysosome
AP1B1	Lysosome
ARSA	Lysosome
AP4S1	Lysosome
LGMN	Lysosome
CTSZ	Lysosome
GLA	Lysosome
ACP5	Lysosome
CLN5	Lysosome
PLA2G15	Lysosome
NAGPA	Lysosome
GGA2	Lysosome
AP3B2	Lysosome
CTSH	Lysosome
LAPTM4B	Lysosome
ASAH1	Lysosome
MAN2B1	Lysosome
DNASE2	Lysosome
ATP6V0A4	Lysosome
AP1S1	Lysosome
LIPA	Lysosome
NAGLU	Lysosome
MANBA	Lysosome

CTSC	Lysosome
TCIRG1	Lysosome
SLC11A2	Lysosome
GNPTAB	Lysosome
ARSB	Lysosome
HYAL1	Lysosome
ATP6V0B	Lysosome
CTSD	Lysosome
NPC2	Lysosome
SLC17A5	Lysosome
CLTA	Lysosome
GGA3	Lysosome
IDUA	Lysosome
CD68	Lysosome
AP1M2	Lysosome
PPT1	Lysosome
NAPSA	Lysosome
AP3B1	Lysosome
SORT1	Lysosome
AP4B1	Lysosome
ACP2	Lysosome
CTSL	Lysosome
CD63	Lysosome
CD164	Lysosome
GNS	Lysosome
CTSV	Lysosome
DNASE2B	Lysosome
SCARB2	Lysosome
GALNS	Lysosome
ARSG	Lysosome
CLTC	Lysosome
NPC1	Lysosome
CTSK	Lysosome
SUMF1	Lysosome
ATP6V0D2	Lysosome
ABCB9	Lysosome
AP1S3	Lysosome
AP3S2	Lysosome
ATP6V0D1	Lysosome
LAPTM5	Lysosome

CTSS	Lysosome
MFSD8	Lysosome
CTSB	Lysosome
HGSNAT	Lysosome
SMPD1	Lysosome
TPP1	Lysosome
AP1G1	Lysosome
GUSB	Lysosome
GLB1	Lysosome
GAA	Lysosome
CTSW	Lysosome
CTSF	Lysosome
CLTB	Lysosome
GBA	Lysosome
AP3S1	Lysosome
PSAPL1	Lysosome
FUCA1	Lysosome
SGSH	Lysosome
AP1S2	Lysosome
AP3M1	Lysosome
ATP6V0A2	Lysosome
ATP6V0C	Lysosome
LAMP1	Lysosome
CLN3	Lysosome
CTSE	Lysosome
GM2A	Lysosome
IGF2R	Lysosome
ENTPD4	Lysosome
PSAP	Lysosome
NAGA	Lysosome
NEU1	Lysosome
HEXA	Lysosome
AP4M1	Lysosome
PPT2	Lysosome
CTSO	Lysosome
PFKP	Glycolysis
PKM	Glycolysis
ENO1	Glycolysis
PGK1	Glycolysis
GPI	Glycolysis

GAPDH	Glycolysis
TPI1	Glycolysis
LDHA	Glycolysis
PFKL	Glycolysis
ALDOA	Glycolysis
HK1	Glycolysis
PGAM1	Glycolysis
SLC25A13	Mitochondrial Biogenesis
SLC25A5	Mitochondrial Biogenesis
COX10	Mitochondrial Biogenesis
BID	Mitochondrial Biogenesis
TOMM34	Mitochondrial Biogenesis
MIPEP	Mitochondrial Biogenesis
BAK1	Mitochondrial Biogenesis
SLC25A3	Mitochondrial Biogenesis
HSP90AA1	Mitochondrial Biogenesis
SLC25A24	Mitochondrial Biogenesis
DNM1L	Mitochondrial Biogenesis
SH3GLB1	Mitochondrial Biogenesis
SLC25A1	Mitochondrial Biogenesis
TOMM22	Mitochondrial Biogenesis
TSPO	Mitochondrial Biogenesis
SLC25A17	Mitochondrial Biogenesis
TIMM9	Mitochondrial Biogenesis
SLC25A14	Mitochondrial Biogenesis
TAZ	Mitochondrial Biogenesis
SLC25A15	Mitochondrial Biogenesis
TIMM44	Mitochondrial Biogenesis
TIMM50	Mitochondrial Biogenesis
BBC3	Mitochondrial Biogenesis
UCP1	Mitochondrial Biogenesis
GRPEL1	Mitochondrial Biogenesis
AIP	Mitochondrial Biogenesis
SOD2	Mitochondrial Biogenesis
SLC25A12	Mitochondrial Biogenesis
MFN2	Mitochondrial Biogenesis
SLC25A2	Mitochondrial Biogenesis
SLC25A16	Mitochondrial Biogenesis
SLC25A19	Mitochondrial Biogenesis
MSTO1	Mitochondrial Biogenesis

SLC25A23	Mitochondrial Biogenesis
UXT	Mitochondrial Biogenesis
TIMM17B	Mitochondrial Biogenesis
RHOT1	Mitochondrial Biogenesis
TIMM8A	Mitochondrial Biogenesis
MTX2	Mitochondrial Biogenesis
TOMM40	Mitochondrial Biogenesis
STARD3	Mitochondrial Biogenesis
TIMM10B	Mitochondrial Biogenesis
TIMM17A	Mitochondrial Biogenesis
TIMM10	Mitochondrial Biogenesis
LRPPRC	Mitochondrial Biogenesis
RHOT2	Mitochondrial Biogenesis
PMAIP1	Mitochondrial Biogenesis
SOD1	Mitochondrial Biogenesis
HSPD1	Mitochondrial Biogenesis
SLC25A37	Mitochondrial Biogenesis
CDKN2A	Mitochondrial Biogenesis
SLC25A25	Mitochondrial Biogenesis
IMMP1L	Mitochondrial Biogenesis
TIMM8B	Mitochondrial Biogenesis
SLC25A31	Mitochondrial Biogenesis
SLC25A4	Mitochondrial Biogenesis
SLC25A27	Mitochondrial Biogenesis
CPT2	Mitochondrial Biogenesis
TOMM40L	Mitochondrial Biogenesis
COX18	Mitochondrial Biogenesis
MFN1	Mitochondrial Biogenesis
BCL2L1	Mitochondrial Biogenesis
BCL2	Mitochondrial Biogenesis
TOMM20	Mitochondrial Biogenesis
SLC25A30	Mitochondrial Biogenesis
UCP3	Mitochondrial Biogenesis
UCP2	Mitochondrial Biogenesis
SFN	Mitochondrial Biogenesis
BNIP3	Mitochondrial Biogenesis
TIMM22	Mitochondrial Biogenesis
SLC25A22	Mitochondrial Biogenesis
SLC25A20	Mitochondrial Biogenesis
SLC25A21	Mitochondrial Biogenesis

SLC25A10	Mitochondrial Biogenesis
IMMP2L	Mitochondrial Biogenesis
OPA1	Mitochondrial Biogenesis
CPT1B	Mitochondrial Biogenesis
DNAJC19	Mitochondrial Biogenesis
FIS1	Mitochondrial Biogenesis

Table S2. Antibodies used for RPPA Analysis

Antibody	Vendor	Catalogue number	Dilution
4E-BP1 (S65)	Cell Signaling Technologies	9451	1:50
4E-BP1 (T37/46)	Cell Signaling Technologies	9459	1:100
4E-BP1 (T70)	Cell Signaling Technologies	9455	1:200
Acetyl-CoA Carboxylase (S79)	Cell Signaling Technologies	3661	1:50
Akt	Cell Signaling Technologies	9272	1:2000
Akt (S473)	Cell Signaling Technologies	9271	1:100
Akt (T308)	Cell Signaling Technologies	9275	1:100
Akt1/PKB alpha (S473) (SK703)	Upstate	05-736	1:100
Aldehyde Dehydrogenase 2 (ALDH2)	Abcam	ab54828	1:100
AMPKalpha (T172) (D79.5E)	Cell Signaling Technologies	4188	1:2000
AMPKBeta1 (S108)	Cell Signaling Technologies	4181	1:50
Androgen Rec (S650)	Abcam	ab47563	1:1000
Androgen Rec (S81)	Millipore	07-1375	1:1000
A-Raf (S299)	Cell Signaling Technologies	4431	1:50
ASK1 (S83)	Cell Signaling Technologies	3761	1:50
ATF-2 (T71)	Cell Signaling Technologies	9221	1:100
Atg5	Cell Signaling Technologies	2630	1:1000
ATR (S428)	Cell Signaling Technologies	2853	1:50
Aurora A (T288)/B (T232)/C (T198) (D13A11)	Cell Signaling Technologies	2914	1:50
Bad	Cell Signaling Technologies	9292	1:1000
BAD (S112)	Cell Signaling Technologies	9291	1:200
Bad (S136)	Cell Signaling Technologies	9295	1:50
Bad (S155)	Cell Signaling Technologies	9297	1:100
Bak	Cell Signaling Technologies	3814	1:100
Bax	Cell Signaling Technologies	2772	1:200
Bcl-2	Cell Signaling Technologies	2872	1:100
Bcl-2 (S70) (5H2)	Cell Signaling Technologies	2827	1:50
Bcl-xL	Cell Signaling Technologies	2762	1:500
Beclin 1	Cell Signaling Technologies	3738	1:100
Biliverdin Reductase (BVR)	Stressgen	OSA-400	1:500
BIM	Cell Signaling Technologies	2933	1:500
BLVRB (biliverdin reductase B) (2F4)	Abnova	H00000645-M09	1:50
B-Raf (S445)	Cell Signaling Technologies	2696	1:50
c-Abl (T735)	Cell Signaling Technologies	2864	1:50
c-Abl (Y245)	Cell Signaling Technologies	2861	1:100

Caspase-3, cleaved (D175)	Cell Signaling Technologies	9661	1:50
Caspase-6, cleaved (D162)	Cell Signaling Technologies	9761	1:50
Caspase-7, cleaved (D198)	Cell Signaling Technologies	9491	1:100
Caspase-9, cleaved (D330)	Cell Signaling Technologies	9501	1:50
Catenin (beta) (S33/37/T41)	Cell Signaling Technologies	9561	1:100
Catenin (beta) (T41/S45)	Cell Signaling Technologies	9565	1:50
Caveolin-1 (Y14) (EPR2288Y)	Epitomics	2267-1	1:200
CDK2 (78B2)	Cell Signaling Technologies	2546	1:200
Chk-1 (S345)	Cell Signaling Technologies	2341	1:50
c-Kit (Y719)	Cell Signaling Technologies	3391	1:100
c-Myc	Cell Signaling Technologies	9402	1:100
Cofilin (S3) (77G2)	Cell Signaling Technologies	3313	1:500
cPLA2 (S505)	Cell Signaling Technologies	2831	1:1000
c-Raf (S338) (56A6)	Cell Signaling Technologies	9427	1:200
CREB (S133)	Cell Signaling Technologies	9191	1:100
CrkII (Y221)	Cell Signaling Technologies	3491	1:100
Cu/Zn Superoxide Dismutase (SOD)	Stressgen	SOD-100	1:750
Cytochrome C oxidoreductase	MitoSciences	MS408	1:250
DEPTOR	Millipore	09-463	1:4000
E-Cadherin	Cell Signaling Technologies	4065	1:500
EGFR (Y1068)	Cell Signaling Technologies	2234	1:50
EGFR (Y1148)	BioSource	44-792	1:100
EGFR (Y1173)	BioSource	44-794	1:100
eIF2alpha (S51) (119A11)	Cell Signaling Technologies	3597	1:500
eIF4E (S209)	Cell Signaling Technologies	9741	1:50
eIF4G (S1108)	Cell Signaling Technologies	2441	1:1000
Elk-1 (S383)	Cell Signaling Technologies	9181	1:100
eNOS (S1177)	Cell Signaling Technologies	9571	1:50
eNOS/NOS III (S116)	Upstate	07-357	1:500
ErbB2/HER2 (Y1248)	Imgenex	IMG-90189	1:500
ErbB3/HER3 (Y1289) (21D3)	Cell Signaling Technologies	4791	1:200
ERCC1 (4F9)	Origene	UM500008	1:50
ERK (T202/Y204)	Cell Signaling Technologies	9101	1:1000
ERK 1/2	Cell Signaling Technologies	9102	1:200
Etk (Y40)	Cell Signaling Technologies	3211	1:2000
Ezrin (T567)/Radixin (T564)/Moesin (T558)	Cell Signaling Technologies	3141	1:100
Ezrin (Y353)	Cell Signaling Technologies	3144	1:100
FADD (S194)	Cell Signaling Technologies	2781	1:100
FAK (Y397) (18)	BD	611806	1:50

FAK (Y576/577)	Cell Signaling Technologies	3281	1:200
FKHR/FOX01 S256	Cell Signaling Technologies	9461	1:100
FKHR-FOX01 T24/FKHRL1-FOX03a T32	Cell Signaling Technologies	9464	1:200
FKHRL1/FOX03 (S253)	Upstate	06-953	1:1000
FOXM1 (T600)	Cell Signaling Technologies	14655	1:100
GSK-3a/B (S21/9)	Cell Signaling Technologies	9331	1:100
GSK-3alpha (S21) (46H12)	Cell Signaling Technologies	9337	1:100
GSK-3alpha (Y279)/beta (Y216)	Biosource	44-604	1:500
GSK-3beta (S9)	Cell Signaling Technologies	9336	1:100
Heme-Oxygenase-1	Stressgen	SPA-894	1:500
Histone H3 (S10) Mitosis Marker	Upstate	06-570	1:200
Histone H3 (S28)	Upstate	07-145	1:1000
HSP90a (T5/7)	Cell Signaling Technologies	3488	1:100
IGF-1 Rec (Y1131)/Insulin Rec (Y1146)	Cell Signaling Technologies	3021	1:500
IGF-1R (Y1135/36)/IR (Y1150/51) (19H7)	Cell Signaling Technologies	3024	1:500
IkappaB-alpha (S32/36) (39A1431)	Cell Signaling Technologies	551818	1:50
IRS-1 (S612)	Cell Signaling Technologies	2386	1:200
LAMP-2 (H4HB4)	SantaCruz	sc-18822	1:2000
LC3B	Cell Signaling Technologies	2775	1:100
Lck (Y505)	Biosource	44-850	1:50
LDHA	Cell Signaling Technologies	2012	1:100
LIMK1 (T508)/LIMK2 (T505)	Cell Signaling Technologies	3841	1:100
LKB1 (S334)	Cell Signaling Technologies	3055	1:50
LKB1 (S428)	Cell Signaling Technologies	3051	1:100
MARCKS (S152/156)	Cell Signaling Technologies	2741	1:200
MDM2 (S166)	Cell Signaling Technologies	3521	1:100
MEK1 (S298)	Cell Signaling Technologies	9128	1:2000
MEK1/2 (S217/221)	Cell Signaling Technologies	9121	1:500
Met (Y1234/1235)	Cell Signaling Technologies	3126	1:200
Mn Superoxide Dismutase (SOD)	Assay Design	SOD-110	1:500
MSK1 (S360)	Cell Signaling Technologies	9594	1:50
Mst1 (T183)/Mst2 (T180)	Cell Signaling Technologies	3681	1:50
mTOR (S2448)	Cell Signaling Technologies	2971	1:100
NF-kappaB p65 (S536)	Cell Signaling Technologies	3031	1:100
p27 (T187)	Zymed	71-7700	1:200
p38 MAPK (T180/Y182)	Cell Signaling Technologies	9211	1:100
p53 (S15)	Cell Signaling Technologies	9284	1:1000
p62/SQSTM1 (D5E2)	Cell Signaling Technologies	8025	1:50

p70 S6 Kinase (S371)	Cell Signaling Technologies	9208	1:50
p70 S6 Kinase (T389)	Cell Signaling Technologies	9205	1:100
p70 S6 Kinase (T412)	Upstate	07-018	1:500
p90RSK (S380)	Cell Signaling Technologies	9341	1:200
PAK1 (T423)/PAK2 (T402)	Cell Signaling Technologies	2601	1:100
PAK2 (S20)	Cell Signaling Technologies	2607	1:100
PARP, cleaved (D214)	Cell Signaling Technologies	9541	1:100
PDK1 (S241)	Cell Signaling Technologies	3061	1:200
PI3-Kinase	BD	610045	1:100
PI3-Kinase p110gamma	Cell Signaling Technologies	4252	1:100
PKA C (T197)	Cell Signaling Technologies	4781	1:200
PKC alpha (S657)	Upstate	06-822	1:1000
PKC delta (T505)	Cell Signaling Technologies	9374	1:50
PKC theta (T538)	Cell Signaling Technologies	9377	1:100
PKC zeta/lambda (T410/403)	Cell Signaling Technologies	9378	1:50
PLC-gamma-1	Cell Signaling Technologies	2822	1:500
PLK1	Cell Signaling Technologies	4535	1:100
PLK1 (T210)	BD	558400	1:200
PRAS40 (T246)	BioSource	44-1100	1:1000
Proteasome 20S C2	Abcam	ab3325	1:500
PTEN	Cell Signaling Technologies	9552	1:50
PTEN (S380)	Cell Signaling Technologies	9551	1:500
PUMA	Cell Signaling Technologies	4976	1:200
Pyk2 (Y402)	Cell Signaling Technologies	3291	1:200
Raf (S259)	Cell Signaling Technologies	9421	1:100
Ras (RAS10)	Millipore	05-516	1:200
Ras-GRF1 (S916)	Cell Signaling Technologies	3321	1:50
Rb (S780)	Cell Signaling Technologies	3590	1:2000
Ret (Y905)	Cell Signaling Technologies	3221	1:100
Ron (Y1353)	Epitomics	5176-1	1:1000
RSK3 (T356/S360)	Cell Signaling Technologies	9348	1:500
S6 Ribosomal Protein (S235/236) (2F9)	Cell Signaling Technologies	4856	1:200
S6 Ribosomal Protein (S240/244)	Cell Signaling Technologies	2215	1:1000
SAPK/JNK (T183/Y185)	Cell Signaling Technologies	9251	1:100
SEK1/MKK4 (S80)	Cell Signaling Technologies	9155	1:50
Shc (Y317)	Upstate	07-206	1:200
Smad2 (S245/250/255)	Cell Signaling Technologies	3104	1:100
Smad2 (S465/467)	Cell Signaling Technologies	3101	1:200
Src (Y527)	Cell Signaling Technologies	2105	1:200

Src Family (Y416)	Cell Signaling Technologies	2101	1:100
ST6GALNAC5	Aviva	ARP49986	1:50
Thioredoxin Reductase 1 (TrxR1)	SantaCruz	sc28321	1:50
Vav3 (Y173)	Biosource	44-488	1:1000
Vimentin	Cell Signaling Technologies	3295	1:500
YAP (S127) (D9W2I)	Cell Signaling Technologies	13008	1:100

Table S3. Antibodies with significant changes in signal at 1 hour

Antibody	p-value (FDR corrected)
p90RSK.S380	0.010811942
RSK3.T356.360	0.010811942
MDM2.S166	0.010811942
p70S6.Kinase.T412	0.010811942
4EBP1.T70	0.010811942
Akt1.PKB.alpha.S473	0.010811942
FKHR.FOX01.T24.FKHRL1.FOX03a.T32	0.010811942
cPLA2.S505	0.012613932
MEK.1.2.S217.221	0.012613932
BAD.S112	0.012613932
ATF.2.T71	0.012613932
HSP90a.T5.7	0.012613932
ERK.1.2.T202.Y204	0.02328726
p70S6.Kinase.T389	0.023651123
eIF4E.S209	0.023651123
AKT.S473	0.023651123
AMPKalpha.T172	0.042046441
ErbB3.HER3.Y1289	0.042046441

PDAC cell lines were treated with vehicle (DMSO) or SCH772984 (ERKi, 1 μM) for 1 or 24 h. Three independent experiments were prepared and reverse-phase protein array (RPPA) analysis was performed. RPPA expression data for 1 h of SCH772984 treatment were standardized to no treatment samples. Data were log2 transformed and medians of three independent experiments are represented in the heat map. Only proteins with statistically significant ($p < 0.05$, FDR corrected, Wilcoxon test) changes at 1 h are shown.

Table S4. Antibodies with significant changes in signal at 24 hours

Antibody	p-value (FDR corrected)
p90RSK.S380	0.004730225
RSK3.T356.360	0.004730225
MDM2.S166	0.004730225
p70S6.Kinase.T412	0.004730225
cPLA2.S505	0.004730225
ERK.1.2.T202.Y204	0.004730225
AMPKalpha.T172	0.004730225
Cofilin.S3	0.004730225
mTOR.S2448	0.004730225
4EBP1.S65	0.004730225
Raf.S259	0.004730225
c.Myc	0.004730225
CREB.S133	0.004730225
PLK1	0.004730225
SAPK.JNK.T183.185	0.004730225
eNOS.NOS.III.S116	0.004730225
S6.Ribosomal.Protein.S240.244	0.004730225
Ron.Y1353	0.004730225
ERK.1.2.TOTAL	0.004730225
GSK.3a.B.S21.9	0.004730225
eIF4G.S1108	0.004730225
GSK.3beta.S9	0.004730225
ATR.S428	0.004730225
YAP.S127	0.004730225
FADD.S194	0.004730225
PI3.Kinase	0.004730225
Mn.Superoxide.Dismutase	0.004730225
BIM	0.004730225
Rb.S780	0.004730225
S6.Ribosomal.Protein.S235.236	0.004730225
AR.S81	0.004730225
Heme.Oxygenase.1	0.004730225
PARP.cleaved.D214	0.006880327
IRS.1.S612	0.008649554
BLVRB..Biliverdin.Reductase.B.	0.008649554
MEK.1.2.S217.221	0.009958368
Caspase.7.Cleaved.D198	0.009958368
GSK.3alpha.Y279.beta.Y216	0.009958368

FAK.Y397	0.01164363
Acetyl.CoA.Carboxylase.S79	0.013244629
PUMA	0.014415923
Ras..RAS10.	0.014415923
Chk.1.S345	0.016102892
CDK2	0.016102892
MARCKS.S152.156	0.016102892
Catenin.beta.S33.37.T41	0.016102892
Bcl.2	0.016102892
MSK1.S360	0.021191406
FKHR.FOX01.S256	0.021191406
Histone.H3.S28	0.021191406
p70S6.Kinase.T389	0.027521307
Bcl.xL	0.027521307
IGF.1.Rec.Y1131.IR.Y1146	0.027521307
PKC.alpha.S657	0.027521307
LAMP.2	0.027521307
ERCC1	0.037177906
FOXM1.T600	0.037177906
ALDH2	0.038570478
4EBP1.T70	0.040283203
Lck.Y505	0.040283203
Elk.1.S383	0.040283203
PLC.gamma.1	0.040283203
Cytochrome.C.oxidoreductase	0.045650422
PTEN.TOTAL	0.047302246
Ras.GRF1.S916	0.049309008
p27.T187	0.049309008

PDAC cell lines were treated with vehicle (DMSO) or SCH772984 (ERKi, 1 μM) for 1 or 24 h. Three independent experiments were prepared and reverse-phase protein array (RPPA) analysis was performed. RPPA expression data for 24 h SCH772984 treatment samples were standardized to 24 h DMSO treated samples. Data were log2 transformed and medians of three independent experiments are represented in the heat map. Only proteins with statistically significant ($p < 0.05$, FDR corrected, Wilcoxon test) changes 24 h are shown.